

Extrinsic and intrinsic apoptosis activate Pannexin-1 to drive NLRP3 inflammasome assembly

Kaiwen W. Chen^{1,4}, Benjamin Demarco^{1,4}, Rosalie Heilig¹, Kateryna Shkarina¹, Andreas Boettcher², Christopher J. Farady², Pawel Pelczar³, Petr Broz^{1,*}

¹Department of Biochemistry, University of Lausanne, CH-1066 Epalinges, Switzerland

² Novartis Institutes for BioMedical Research Forum 1, Basel, Switzerland

³Center for Transgenic Models, University of Basel, Basel, Switzerland

⁴These authors contributed equally

*Corresponding author: petr.broz@unil.ch

Abstract

Pyroptosis is a form of lytic inflammatory cell death driven by inflammatory caspases-1, -4, -5 and -11. These caspases cleave and activate the pore-forming protein gasdermin D (GSDMD) to induce membrane damage¹⁻³. By contrast, apoptosis is driven by apoptotic caspase-8 or -9 and has traditionally been classified as an immunologically silent form of cell death. Emerging evidence suggest that clinical inhibitors designed for cancer chemotherapy or inflammatory disorders such as SMAC mimetic, TAK1 inhibitors and BH-3 mimetic promote caspase-8 or -9-dependent inflammatory cell death and NLRP3 inflammasome activation⁴⁻⁸. However, the mechanism by which caspase-8 or -9 triggers cell lysis and NLRP3 activation is still undefined. Here, we demonstrate that during extrinsic apoptosis, caspase-8 cleaves GSDMD to promote lytic cell death. By engineering a novel GSDMD D88A knock-in mouse, we further demonstrate that this proinflammatory function of caspase-8 is counteracted by caspase-3-dependent cleavage and inactivation of gasdermin D at Aspartate 88, and is essential to suppress GSDMD-dependent cell lysis during caspase-8-dependent apoptosis. Lastly, we provide evidence that channel-forming glycoprotein pannexin-1, but not GSDMD or GSDME promote NLRP3 inflammasome activation during caspase-8 or -9-dependent apoptosis.

Main

Gasdermin D (GSDMD) is a novel pore-forming protein that is emerging as an important player in cell death and inflammation, particularly during inflammasome and pyroptosis signalling. In macrophages and dendritic cells, cleavage of GSDMD at Aspartate 276 (D276) by inflammasome-activated inflammatory caspases (e.g. caspase-1, caspase-4, caspase-5, caspase-11) liberates the cytotoxic p30 N-terminal domain to generate plasma membrane pores and drive pyroptosis^{1-3,9-12}; while GSDMD cleavage by caspase-4, caspase-11 or neutrophil elastase promotes extrusion of neutrophil extracellular traps^{13,14}. By contrast, GSDMD cleavage at position Aspartate 88 (D88) by apoptotic caspase-3 inactivates the pyroptotic properties of GSDMD¹⁵, indicating that GSDMD may be activated by inflammasome-

independent mechanisms during apoptosis. To investigate whether GSDMD promotes cell lysis during extrinsic apoptosis, we stimulated wild type (WT) or *Gsdmd*^{-/-} bone marrow-derived macrophages (BMDM) with TNF in combination with the SMAC mimetic AZD5582 (hereafter referred as SM) or the TAK1 inhibitor 5z-7-oxozeaenol (hereafter referred as TAK1i), to induce the assembly of the ripoptosome, a caspase-8-activating platform^{6,16-18}. Surprisingly, caspase-8 activation triggered GSDMD-dependent cell lysis (**Fig. 1A-B**) and induced hallmarks of pyroptosis including membrane ballooning and uptake of the membrane-impermeable dye propidium iodide (PI) in WT macrophages (**Fig. 1C; black arrow head; Supplementary Video 1**). By contrast, *Gsdmd*-deficient cells retained membrane integrity and displayed classical apoptotic morphology such as cell shrinkage and the release of apoptotic bodies (**Fig 1C; white arrow head; Supplementary Video 2**). However, *Gsdmd* deficiency did not completely protect macrophages from caspase-8-dependent cell lysis (**Fig. 1A-B**); and *Gsdmd*-deficient apoptotic bodies incorporate PI over time (**Fig 1C; white arrow head**). Therefore, we investigate whether GSDMD-independent cell lysis is driven by caspase-3 and/or -7-dependent secondary necrosis. To investigate this possibility, we deleted *caspase-3*, *caspase-7* or *caspase-3 and -7* in *Gsdmd*^{-/-} immortalized BMDMs (iBMDM) using CRISPR-Cas9 technology and stimulated these cells with TNF and SM or TAK1i. Indeed, *Gsdmd*^{-/-}*Casp3*^{-/-}, *Gsdmd*^{-/-}*Casp7*^{-/-} and *Gsdmd*^{-/-} *Casp3/7*^{-/-} iBMDMs were resistant to cell lysis following caspase-8 activation (**Fig. 1D-E**). Taken together, our data indicate that extrinsic apoptosis promotes GSDMD-dependent cell lysis in parallel with caspase-3/7-dependent secondary necrosis.

Since caspase-8 activation may indirectly promote GSDMD cleavage by activating the NLRP3 inflammasome^{6,18,19}, we next investigated cell death and GSDMD processing in WT versus inflammasome-deficient BMDM. Indeed, we observed that *Nlrp3*, *Asc*, *Caspase-1/11* deficiency similarly reduced TNF and SM or TAK1i-induced cell death (**Fig. 2A; Supplementary Fig. 1A**). Unexpectedly, *Gsdmd*^{-/-} BMDMs were even more protected than *Nlrp3*^{-/-} and *Caspase-1/11*^{-/-} BMDM following TNF and TAK1i stimulation (**Fig. 2A**), suggesting that GSDMD may be activated by caspase-1-dependent and

independent pathways. Consistent with that, we observed robust GSDMD processing into the active p30 and the appearance of an inactive p20 fragment, resulting from an inactivation cleavage by caspase-3 at position D88, in WT, *Nlrp3* and *Caspase-1/11*-deficient primary or immortalized BMDM after stimulation with TNF or LPS in combination with SM or TAK1i (**Fig. 2B-C; Supplementary Fig. 1B-C**). Caspase-8 triggers NLRP3 activation through a potassium efflux-dependent mechanism²⁰, suggesting that caspase-8 likely triggers NLRP3 assembly by inducing plasma membrane damage. We therefore hypothesize that caspase-1/11-independent GSDMD activation promotes plasma membrane pore formation, potassium efflux and NLRP3 activation, analogous to NLRP3 activation by the non-canonical inflammasome^{21,22}. However, TNF or LPS co-stimulated with SM or TAK1i induced comparable levels of caspase-1 p20 autoprocessing, a hallmark of inflammasome activation, between WT and *Gsdmd*^{-/-} macrophages (**Fig. 2B, 2D, 2E, 2G; Supplementary Fig 1D-E**); and extracellular potassium similarly reduced caspase-1 processing in WT and *Gsdmd*^{-/-} BMDMs (**Fig. 2D-E**). Gasdermin E (GSDME), another pyroptotic effector from the Gasdermin protein family, is activated by caspase-3 during apoptosis and proposed to mediate secondary necrosis in BMDMs^{23,24}. Consistent with previous reports, we observed robust GSDME processing into the active p30 fragment during apoptosis, however, *Gsdme*-deficiency did not reduce cell death or caspase-1 processing in WT or *Gsdmd*^{-/-} macrophages (**Fig. 2F-G; Supplementary Fig. 1F**), indicating that caspase-8 triggers potassium efflux and NLRP3 activation through GSDMD or GSDME-independent pores.

Since we observed that GSDMD processing is ablated in *Ripk3*^{-/-}*Casp8*^{-/-} during extrinsic apoptosis (**Supplementary Fig. 2A**), and caspase-1 and caspase-8 recognize and cleave overlapping sequences in substrates such as pro-IL-1 β ⁶, we hypothesized that caspase-8 could directly trigger GSDMD activation. For this, we engineered a doxycycline-inducible caspase-8 construct, in which we replaced the DED domains of caspase-8 with a DmrB domain to control caspase-8 dimerization upon addition of the B/B homodimerizer drug. Next, we ectopically expressed DmrB-caspase-8 with

WT full-length GSDMD, a caspase-1/11-uncleavable D276A mutant, a caspase-3-uncleavable D88A mutant and a D88A D276A double mutant in HEK293T cells which are naturally deficient in caspase-1 (**Supplementary Fig. 2B**). Indeed, addition of doxycycline and B/B homodimerizer to induce caspase-8 expression and dimerization triggered cleavage of WT GSDMD into the active p30 fragment and the appearance of the inactive p43 and p20 fragments, corresponding to cleavage of full-length GSDMD or further processing of active p30 at position D88 by caspase-3 (**Fig. 3A, 2C**). Consistent with that, we observed an accumulation of active p30 and complete disappearance of the inactive p43 and p20 fragment in the D88A mutant. Conversely, caspase-8 dimerization triggered an accumulation of the inactive p43 but not the appearance of active p30 and inactive p20 when D276 was mutated, indicating that caspase-8 and caspase-1 can process GSDMD at the same residue (**Fig. 3A**); consistent with a recent report that caspase-8 triggers direct GSDMD during *Yersinia* infection²⁵. To verify *in vitro* that human caspase-1 and -8 cleave GSDMD at the same residue, we designed a GSDMD-based substrate derived from the caspase-1 cleavage site in GSDMD and monitored its cleavage using a fluorometric assay (**Supplementary Fig. 2C**). Indeed, human caspase-8 processed the GSDMD-based substrate, though 30-fold less efficiently than caspase-1 (**Supplementary Fig. 2D-E**). Since caspase-3 is activated downstream of caspase-8 during apoptosis, we next investigated whether the direct caspase-8-dependent GSDMD activation is counteracted by caspase-3-dependent GSDMD inactivation at position D88. For this, we reconstituted immortalized *Gsdmd*^{-/-} BMDMs with either WT GSDMD (GSDMD^{WT}) or a caspase-3-uncleavable D88A mutant (GSDMD^{D88A}) by lentiviral transduction and monitored cell death after TNF and SM or LPS and LCL161 (smac mimetic)-induced caspase-8 activation. Remarkably, GSDMD^{D88A}-expressing iBMDMs were significantly more susceptible than GSDMD^{WT}-expressing controls to both TNF and LPS-induced apoptosis (**Fig. 3B-C**). To investigate whether GSDMD inactivation at D88 is observed in primary macrophages, we generated a GSDMD^{D88A} knock-in mouse. *Gsdmd*^{D88AKI/KI} animals were born at expected Mendelian ratio, healthy and developed a normal immune response (**Supplementary Fig. 3A-F**). Indeed, we observed an accumulation

of the cytotoxic GSDMD p30 fragment and the disappearance of the inactive p20 fragment upon TNF and TAK1i or SM stimulation of *Gsdmd*^{D88AKI/KI} cells, which correlated with a 1.5-fold enhancement in cell death (**Fig. 3D-E; Supplementary Fig. 4A-B**). Although the cytotoxic GSDMD p30 fragment was significantly enriched in *Gsdmd*^{D88AKI/KI} cells compared to WT littermates, caspase-1 processing was unchanged between *Gsdmd*^{D88AKI/KI} and WT littermate controls (**Fig. 3D; Supplementary Fig. 4B**), reiterating that GSDMD pores do not promote caspase-8-dependent NLRP3 activation.

Since the RIPK1 kinase inhibitor Nec-1s suppressed caspase-8-mediated cell death^{4,5,16} (**Fig. 4A**), and RIPK1 signalling is often associated with RIPK3, we next investigated the role of RIPK3 in promoting cell death and NLRP3 activation during TNF-induced apoptosis. RIPK3 did not contribute to TNF and TAK1i-induced cell lysis and GSDMD activation (**Fig. 4B-C**); however, caspase-1 processing was remarkably reduced in *Ripk3*^{-/-} compared to WT macrophages. Extracellular potassium and the NLRP3 specific inhibitor MCC950 reduced GSDMD and processing in WT but not *Ripk3*^{-/-} cells, confirming that RIPK3 is indeed upstream of NLRP3 during TNF-induced apoptosis (**Fig. 4C**). RIPK3 kinase activity can drive NLRP3 activation by promoting MLKL pore formation and potassium efflux^{20,26}. However, TNF and TAK1i did not trigger RIPK3-dependent MLKL phosphorylation (**Fig. 4C**) and *Mkl* did not contribute to cell death or caspase-1 processing (**Supplementary Fig. 5A-B**). In agreement with a RIPK3 kinase-independent role for driving NLRP3 activation, the RIPK3 kinase inhibitor GSK'872 did not suppress cell lysis (**Supplementary Fig. 5C**) but paradoxically promoted caspase-1 processing (**Fig. 4C**), most probably through altering ripoptosome conformation²⁷. Consistent with previous reports, we observed that it is the RIPK3 scaffolding function that promotes ripoptosome-mediated caspase-3 activation (**Fig. 4D**)^{6,17}. Since both caspase-3 and caspase-1 activation was reduced in *Ripk3*^{-/-} cells, we hypothesized that ripoptosome-induced caspase-3 activity drives potassium efflux and NLRP3 activation. Pannexin-1, a channel-forming glycoprotein, is cleaved by caspase-3 during apoptosis²⁸ and pannexin-1 activation can promote membrane permeability and potassium efflux²⁹. We therefore investigated if the ripoptosome promotes

pannexin-1 activity for NLRP3 assembly by using two well-established pannexin-1 inhibitors, probenecid³⁰ and the antibiotic trovafloxacin³¹. Remarkably, probenecid and trovafloxacin strongly reduced caspase-1 activation during TNF-induced apoptosis (**Fig. 4E; Supplementary Fig. 6A**). By contrast, both inhibitors had no effect on caspase-1 processing following nigericin or poly(dAdT) stimulation to activate NLRP3 or AIM2 inflammasome respectively (**Fig. 4E, Supplementary Fig. 6B-C**). Consistent with the role of pannexin-1 in driving caspase-8-dependent NLRP3 activation following TNFR1 engagement, probenecid similarly reduced caspase-1 processing in LPS and SM-stimulated cells (**Fig. 4F**), indicating that the ripoptosome promotes pannexin-1 activity to drive NLRP3 assembly upon TNFR1 and TLR4 stimulation. To validate genetically that Pannexin-1 drives NLRP3 activation upon ripoptosome activation, we stimulated WT and *Panx1*^{-/-} BMDMs with TNF and SM or TAK1i. Consistent with our inhibitor data (**Fig. 4E-F, Supplementary Fig. 6A**), *Panx1* deficiency dramatically reduced caspase-1 processing compared to WT cells upon TNF and SM treatment (**Fig. 4G; Supplementary Fig. 7A**). In line with the requirement for NLRP3 to amplify inflammatory cell death during caspase-8 activation (**Fig. 2A, Supplementary Fig. 1A**), *Panx1* deficiency significantly reduced cell lysis and GSDMD processing following TNF/SM treatment (**Fig. 4G-H**). Interestingly, while caspase-1 processing was reduced in *Panx1*^{-/-} compared to WT BMDMs, it was not sufficient to reduce TNF or LPS and TAK1i-induced cell lysis (**Supplementary Fig. 7A-C**), possibly due to compensatory mechanisms from caspase-8-dependent GSDMD cleavage (**Fig. 2B**) and caspase-3/7-dependent secondary necrosis during TAK1 inhibition (**Fig. 1E**).

Having established that extrinsic apoptosis triggers GSDMD-dependent cell lysis and pannexin-1-dependent NLRP3 activation, we next investigate whether the same pathway occurs during intrinsic apoptosis. For this, we stimulated WT or *Gsdmd*^{-/-} BMDM with a combination of the BH3-mimetic ABT-737 and the MCL-1 inhibitor S63845 to activate mitochondrial apoptosis. ABT-737 and S63845 co-treatment triggered cell lysis over time, however, in contrast to extrinsic apoptosis (**Fig. 1A, B**), ABT-737/S63845-induced cell lysis was GSDMD-independent (**Fig. 5A, B**). In agreement with that, BMDMs

derived from *Gsdmd*^{D88AKI/KI} mice, in which GSDMD cannot be inactivated by caspase-3 did not display an enhancement in cell lysis upon ABT-737/S63845 treatment (**Fig. 5C**). Caspase-3 is activated during mitochondrial apoptosis, and a recent study reported that caspase-3-dependent GSDME activation drives secondary necrosis in BMDMs ²³. In agreement with our earlier data (**Fig. 2G**), ABT-737/S63845 also triggered robust GSDME processing into the active p30 fragment (**Fig. 5D**), however, GSDME p30 did not contribute to mitochondrial apoptosis-induced cell lysis, since intracellular LDH release was GSDME-independent (**Fig. 5E**). Gasdermin pores may promote potassium efflux to activate NLRP3 during intrinsic apoptosis, however, consistent with earlier observations (**Fig. 2B, D, E, G; Supplementary Fig. 1D, E**), caspase-1 processing was comparable between WT, *Gsdmd*^{-/-}, *Gsmde*^{-/-} or *Gsdmd*^{-/-} *Gsmde*^{-/-} BMDMs, indicating that NLRP3 assembly is driven by GSDMD or GSDME-independent mechanisms (**Fig. 5F**). Since caspase-8-dependent NLRP3 activation is pannexin-1-dependent (**Fig. 4G**), we examined whether pannexin-1 similarly promotes NLRP3 activation during mitochondrial apoptosis. Caspase-1 processing was remarkably reduced in LPS-primed and unprimed *Panx1*^{-/-} BMDMs compared to WT cells (**Fig. 5G; Supplementary Fig. 7D**). Given that caspase-1 and -8 both promotes pro-IL-1 β cleavage during apoptosis ^{32,33}, *Panx1*-deficiency only partially reduced IL-1 β secretion into the cell culture supernatant compared to WT cells (**Fig. 5H**).

Here, we demonstrate that during extrinsic apoptosis caspase-8 directly cleaves GSDMD to initiate inflammatory cell death that this is further amplified by the NLRP3 inflammasome. In contrast, the closely related gasdermin family member, GSDME, is dispensable for macrophage cell lysis downstream of the ripoptosome (**Supplementary Fig. 8**). A recent study proposed that caspase-8-dependent GSDMD activation triggers plasma membrane pores and potassium efflux to activate the NLRP3 inflammasome ²⁵. However, we observed that *Gsdmd* deficiency did not impact caspase-1 processing upon caspase-8 activation; and extracellular potassium similarly reduced caspase-1 processing in both WT and *Gsdmd*-deficient cells. In addition, by generating a novel *Gsdmd*^{D88AKI/KI} mouse, we provide unprecedented genetic evidence that accumulation of GSDMD p30 pores

upon caspase-8 activation do not enhance caspase-1 cleavage. Instead, we propose that RIPK3 scaffolding function promotes apoptotic caspase activation, Pannexin-1 activity and potassium efflux downstream of the ripoptosome to trigger NLRP3 inflammasome activation (**Supplementary Fig. 7**). In line with this, we also provide evidence that gasdermins do not promote macrophage cell lysis or NLRP3 activation during mitochondrial apoptosis. Instead, our data indicate that pannexin-1 is a universal requirement for both intrinsic and extrinsic apoptosis to drive NLRP3 activation (**Supplementary Fig. 8**).

While GSDMD promotes pathogenesis independently of cytokine processing in murine models of endotoxin shock ¹, it is unclear whether side effects associated with clinical inhibitors (such as TAK1i and others) are a result of cell death, cytokine processing, or both. Therefore, future studies should investigate if GSDMD ¹⁴ or NLRP3 inhibition can reduce side effects of such clinical inhibitors. Lastly, our finding that trovafloxacin, an antibiotic with known safety concerns ³⁴, blocks NLRP3 inflammasome activation during apoptosis suggests that additional studies should be performed to ensure the safe usage of these drugs in the clinic.

Methods

Mice

All experiments were performed with approval from the veterinary office of the Canton de Vaud and according to the guidelines from the Swiss animal protection law (license VD3257). C57BL/6J mice were purchased from Janvier Labs (France) and housed at specific-pathogen free facility at the University of Lausanne. *Nlrp3*^{-/-}, *Asc*^{-/-}, *Caspase-1/11*^{-/-}, *Gsdmd*^{-/-}, *Ripk3*^{-/-}, *Ripk3*^{-/-}*Casp8*^{-/-}, *Mlkl*^{-/-} and *Panx1*^{-/-} mice have been previously described. *Gsdme*^{-/-} and *Gsdmd*^{D88AKI/KI} mice were generated at Center for Transgenic model of the University of Basel using CRISPR/Cas9 genome targeting as follows: *Gsdme*^{-/-}: Guide RNAs targeting exon 2 of the mouse *Gsdme* gene were designed using gRNA sequence (including PAM) ACTCTTCGTTTGAACCCTGAGG. Injection of the gRNAs and Cas9 protein

into C57BL/6 embryos was done according to standard methods. Biopsies for genotyping were taken at an age of 10–12 days. DNA extraction was performed using the KAPA HotStart Mouse Genotyping Kit according to the manufacturer's protocol. Genotyping PCR was done using Q5 Polymerase (NEB) using primers GSDME_ex2_fw2; (CTGCCCATGACAAGTGGT) and GSDME_ex_rv2 (AGGGCAGTTACAGGAGCCTA), which were designed using Primer3 v.0.4.0 giving a fragment of 529 bp. The mutation was identified as a 1 bp insertion in exon 2 of *Gsdme* resulting in a premature stop codon. *GSDMD^{D88AKI/KI}*: Guide RNAs targeting exon 2 of the *Gsdmd* gene were designed using gRNA sequence (including PAM) AAGTCTCTGATGTCGTCGATGGG. gRNAs and Cas9 protein were co-injected with a 200nt HDR oligo inducing the following mutations: an AT>CC mutation to affect the D>A change and a silent G>C mutation to kill the PAM sequence. This also created a GCCGGC restriction site (NaeI) to genotype the KI animals. Genotyping PCR was done using primers GSDMD_fw2 (TACAGACGGTTGTGAGCCA) and GSDMD_rv2 (GCTTCCCTCATTCAAGTGCT) giving a fragment of 597 bp. *Gsdmd^{+/-}* *Gsdme^{-/-}* mice were created by crossing *Gsdmd^{+/-}* and *Gsdme^{-/-}* mice.

Cell culture

Bone marrow-derived macrophages were differentiated in DMEM (Gibco) supplement with 20% MCSF (3T3 supernatant), 10% heat-inactivated FCS (Bioconcept), 10 mM HEPES (Bioconcept), penicillin/streptomycin (Bioconcept) and non-essential amino acids (Gibco) and stimulated on day 7-9 of differentiation. Immortalized BMDM were maintained in DMEM (Gibco) supplement with 10% MCSF (3T3 supernatant), 10% heat-inactivated FCS (Bioconcept), 10mM HEPES (Bioconcept) and non-essential amino acids (Gibco). HEK 293T and HeLa cells were cultured in DMEM (Gibco) supplemented with 10 mM HEPES (Bioconcept), non-essential amino acids (Gibco) and 5% or 10% heat-inactivated FCS (Bioconcept) respectively.

Lentiviral transduction of mouse immortalized *Gsdmd^{+/-}* BMDMs

To produce lentiviral particles, 1 x 10⁶ HEK 293T cells were seeded in a 6-well plate and transfected with 2 µg lentiviral plasmid, 2 µg psPax2, and 0.4

µg VSV-G using polyethylenimine (Polysciences Inc) for 6 h. The cell culture media were replaced with fresh DMEM (Gibco) supplemented with 10% MCSF (3T3 supernatant), 10% heat-inactivated FCS (Bioconcept), 10mM HEPES (Bioconcept), non-essential amino acids (Gibco) and 1x penicillin/streptomycin (BioConcept), and lentiviral particles were collected and filtered (0.45 µm) 24 h later. Polybrene (6.25 µg/ml; Merck) was added to the filtered solution and added dropwise to the immortalized *Gsdmd*^{+/-} BMDMs (seeded 1 day before at 5 x 10⁵ cells per 6-well) and cells were spin-infected (2900 rpm, 90 min, 37°C) with these particles and incubated at 37°C with 5% CO₂. 3 days later, cells were split into medium containing puromycin (10 µg /ml, InvivoGen) for selection and used 4 days after selection.

Generation of CRISPR knockouts in immortalized BMDMs

Caspase-3, *Caspase-7* and *Caspase-3/-7*-deficient immortalized BMDM (iBMDM) were generated using the genome editing system Alt-R-Crispr-Cas (IDT) according to the manufacturer's protocol. Briefly, the gene-specific targeting crRNA (*Caspase-7*: GATAAGTGGGCACTCGGTCC TGG, *Caspase-3*: AATGTCATCTCGCTCTGGTA CGG, or TGGGCCTGAAATACCAAGTC AGG) was mixed with the universal RNA oligo tracrRNA to form a gRNA complex (crRNA:tracrRNA). The addition of the recombinant Cas9 nuclease V3 allowed the formation of an RNP complex specific for targeting the *Caspase-3* or *-7* genes. The tracrRNA only or RNP complexes were subsequently reverse-transfected into immortalized *Gsdmd*^{+/-} iBMDM using RNAiMax (Invitrogen). The bulk population was tested for successful gene mutation using the T7 endonuclease digestion assay as follows: Cells were lysed by the Kappa Biosystems kit according to the manufacturer's protocol and genomic DNA flanking the guide RNA (crRNA) binding site were amplified by PCR using gene specific primers (*Caspase-7*: fw: TTGCCTGACCCAAGGTTTGT, rv: CCCAGCAACAGGAAAGCAAC/*Caspase-3*: fw: GTGGGGGATATCGCTGTCAT, rv: TGTGTAAGGATGCGGACTGC). The amplified genomic DNA was used to perform the heteroduplex analysis according to the manufacturer's protocol (IDT). Single clones were derived from the bulk population by limiting dilution

and the absence of protein expression in single clones were verified by immunoblotting.

HEK 293T DmrB-Casp-8 dimerization system

HEK 293T cells were seeded in at 2.5×10^4 cells per well 96-well plate the day prior to transfection. Cells were transfected with 300 ng of plasmid using linear polyethylenimine (900 ng; Polysciences Inc) per well, according to the manufacturer's protocol, in plain DMEM (Gibco) and centrifuged at 300 *g* for 5 min at 37°C. Media were replaced with fresh DMEM 6 h later and supplemented with 10 µg/ml doxycycline (Sigma) for 18 h to induce DmrB-Caspase-8 expression. Cells were exposed with 12.5 nM B/B homodimerizer (Clontech) for 2 h in plain DMEM to induce DmrB-Caspase-8 homodimerization and cell extracts were lysed in boiling lysis buffer and analysed by immunoblotting.

Apoptosis and necroptosis assay

Primary and immortalized BMDM were seeded in 96-well plates at 5×10^4 cells per well a day prior to stimulation. For all macrophage cell stimulation, the cell culture medium was replaced with Opti-MEM (Gibco). Macrophages were treated with ABT-737 (500 nM; Selleckchem) and S63845 (250-1000 nM; Selleckchem) in Opti-MEM (Gibco) to induce mitochondrial apoptosis. Alternatively, cells were simultaneously stimulated with recombinant murine TNF (100 ng/ml; Peprotech) and the SMAC mimetic AZD5582 (250-500 nM; Selleckchem) or the TAK1 inhibitor 5z 7-oxozeaenol (125-250 nM; Sigma) in Opti-MEM (Gibco) to trigger TNF-dependent apoptosis. To trigger TLR4-apoptosis, cell were primed with ultrapure *E. coli* K12 LPS (Invivogen) for 3 h and stimulated with AZD5582 (500 nM) for a further 4 h. To induce LPS-induced necroptosis, cells were treated with Q-VD-OPh (10 µM; Selleckchem) during the last 20 min of LPS priming to block caspase-8 activity. In some experiments, BMDM were treated with MCC950 (10 µM; Sigma), GSK872 (1 µM; Selleckchem), Nec-1s (50 µM; Abcam), Probenecid (1 mM; Sigma) and trovafloxacin (5-10 µM; Sigma) 20-30 min prior to cell stimulation.

Inflammasome assay

Primary BMDM were plated in 96-well plates at 5×10^4 cells per well a day prior to stimulation. Cells were primed with ultrapure *E. coli* K12 LPS (Invivogen) for 4h in Opti-MEM and stimulated with nigericin (10 μ M; Sigma) for 1 h or transfected with 0.2 μ g/well of poly(dA:dT) (InvivoGen) using Polyethylenimine (Polysciences Inc) and centrifuged at 300 g for 5 min at room temperature and incubated for 1 h. Where indicated, cells were treated with Probenecid (1 mM; Sigma) and trovafloxacin (5-10 μ M; Sigma) at the last 20-30 min of priming.

LDH release assay

LDH release into the cell culture supernatant was quantified using CytoTox 96 nonradioactive cytotoxicity assay (Promega) and expressed as a percentage of total cellular LDH (100% lysis).

Western blotting

Cell-free methanol/chloroform-precipitated supernatant were resuspended with cell extracts lysed in boiling lysis buffer (66 mM Tris-Cl pH 7.4, 2% SDS, 10mM DTT, NuPage LDS sample buffer; Thermo Fischer) and separated on 14% polyacrylamide gels. Proteins were transferred onto nitrocellulose membrane using Trans-blot Turbo (Bio-Rad). Antibodies for immunoblot were against GSDMD (EPR19828; Abcam; 1:1000), GSDME (EPR19859; Abcam; 1:1000) caspase-1 p20 (casper-1; Adipogen; 1:1000), full-length caspase-8 (4927; Cell Signaling; 1:1000), cleaved caspase-8 (9429; Cell Signalling; 1:1000), caspase-3 (9662; Cell Signalling; 1:1000), phosphorylated MLKL (EPR9515(2); Abcam; 1:1000), pro-IL-1 β (AF-401-NA, R&D; 1:1000) and alpha-tubulin (DM1A; Abcam; 1:2000).

Live cell imaging

BMDMs were seeded at 2.5×10^4 per well in 8-well tissue culture plates (Ibidi) a day before imaging. Cells were stimulated with TNF (100 ng/ml) and SM (250 nM) in Opti-MEM and cells were stained with propidium iodide (0.5 μ g/ml; Sigma). Images were acquired every 5 min over 6 h using a Zeiss

LSM800 point scanning confocal microscope equipped with 63x Plan-Apochromat NA 1.4 oil objective, Zeiss ESID detector module, LabTek heating/CO₂ chamber and motorized scanning stage.

Statistical analyses

Statistical analyses were performed using Graphpad Prism 7 software. All data sets were analyzed for normality using Shapiro-Wilk normality test. Normally distributed data sets were analyzed using the parametric *t* test whereas non-normally distributed data sets were analyzed using non-parametric Mann-Whitney *t* tests. A two-way ANOVA was used to analyze repeated measures over time. Data were considered significant when **P* ≤ 0.05, ***P* ≤ 0.01, ****P* ≤ 0.001, or *****P* ≤ 0.0001.

Author contributions

K.W.C and B.D designed, performed and analysed all experiments with the exception of confocal microscopy and GSDMD substrate cleavage assay that were performed by K.S, and A.B and C.J.F respectively. R.H generated CRISPR knockouts. P.P generated *Gsdme*^{-/-} and *Gsdmd*^{D88AKI/KI} mice. K.W.C and P.B designed, supervised the study and wrote the paper. P.B oversaw the study.

Conflict of interest statement

A.B and C.J.F are employees of Novartis, Inc.

Acknowledgement

This work was supported by grants from the European Research Council (ERC-2017-CoG – 770988 – InflammCellDeath) to P.B. and a Swiss Government Excellence postdoctoral fellowship (2018.0618) to K.W.C. Microscopy and FACS analysis was performed at the UNIL Core Facilities. We thank Prof. Andy Wullaert, Prof. Wei-Lynn Wong and Prof. Nathalie Rouach for sharing *Ripk3*^{-/-}, *Mlkl*^{-/-} and *Panx1*^{-/-} bone marrow respectively; Prof. Thomas Henry and Aubry Tardivel for sharing *Asc*^{-/-} bone marrow; Dr. James Vince

for discussion on SMAC mimetic, and Cristina Ramon-Barros for technical assistance.

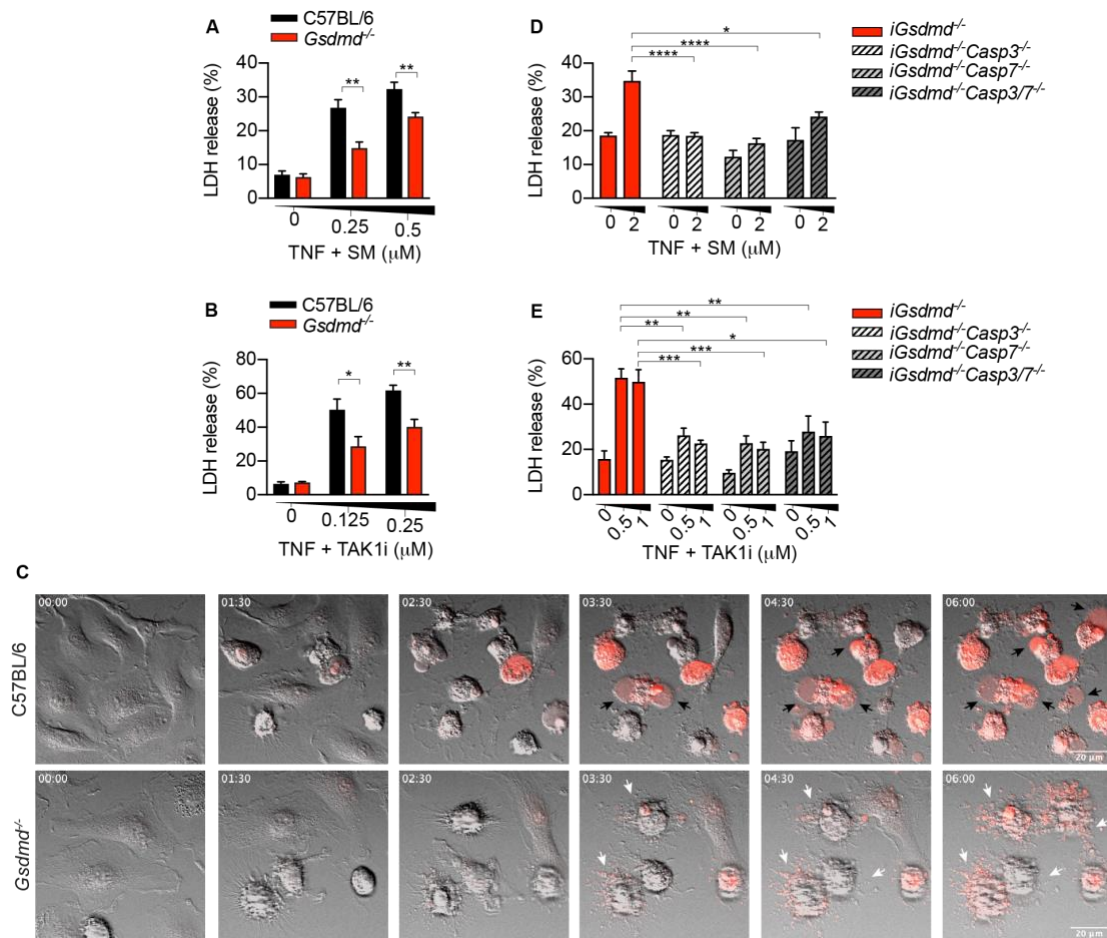


Figure 1. Extrinsic apoptosis trigger GSDMD-dependent and caspase-3/7-dependent necrosis. (A-B) Primary or (D-E) immortalized BMDMs were stimulated with recombinant murine TNF (100 ng/ml) in combination with (A, D) SM or (B, E) TAK1i for 6 or 4 h respectively. (C) Time-lapse confocal images of BMDMs stimulated with recombinant murine TNF (100 ng/ml) and SM (250 nM) stained with propidium iodide (red) for 6 h. Data are means + SEM of pooled data from (A-B) 5 or (D-E) 8 independent experiments. Data were considered significant when $*P < 0.05$ or $**P < 0.01$. (C) Data are representative of 3 independent experiments.

pre-incubated with MCC950 (10 μ M) 20-30 min prior to TNF/TAK1i stimulation. (E-G) BMDMs were costimulated with TNF (100 ng/ml) and SM (E) (250 nM; 6 h) and mixed supernatant and cell extracts were analysed by immunoblot or (F) LDH release in the cell culture supernatant were quantified at the indicated time points. Data are means + SEM of pooled data from (A) 4 or (F) 5 independent experiments. Data were considered significant when $*P<0.05$, $**P<0.01$, $***P<0.001$ or $****P<0.0001$. All immunoblots are representative of 3 independent experiments.

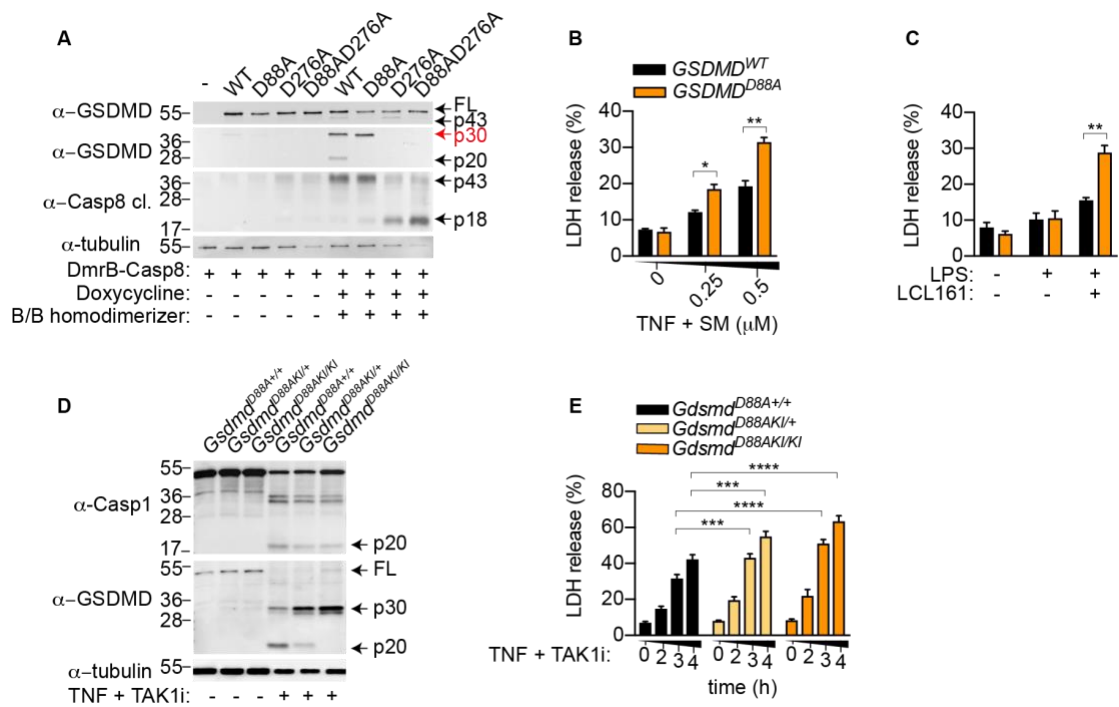


Figure 3. Caspase-3 counteracts caspase-8-dependent GSDMD activation during extrinsic apoptosis. (A) HEK 293T cells were transfected with doxycycline-inducible DmrB-caspase-8 and the indicated GSDMD constructs. Cells were stimulated with doxycycline (10 μ g/ml) for 18 h to induce DmrB-caspase-8 expression and exposed to B/B homodimerizer (12.5 nM) for another 2 h to activate caspase-8. Mixed supernatant and extracts were analysed by immunoblot. (B-C) Immortalized *Gsdmd*^{-/-} BMDMs expressing GSDMD^{WT} and GSDMD^{D88A} were (B) costimulated with TNF (100 ng/ml) and SM for 6 h or (C) primed for 3 h with ultrapure *E. coli* K12 LPS (100 ng/ml) and stimulated with LCL161 (1 μ M) for 24 h and LDH release was quantified. (D-E) BMDMs were costimulated with TNF (100 ng/ml) and TAK1i for 4 h and (D) mixed supernatant and extracts were analysed by immunoblot or (E) LDH release was quantified at the indicated time points. All immunoblots are representative of 3 independent experiments. Data are means +SEM of pooled data from (B-C) 3 or (E) 7 individual experiments. Data were considered significant when * P <0.05, ** P <0.01, *** P <0.001 or **** P <0.0001.

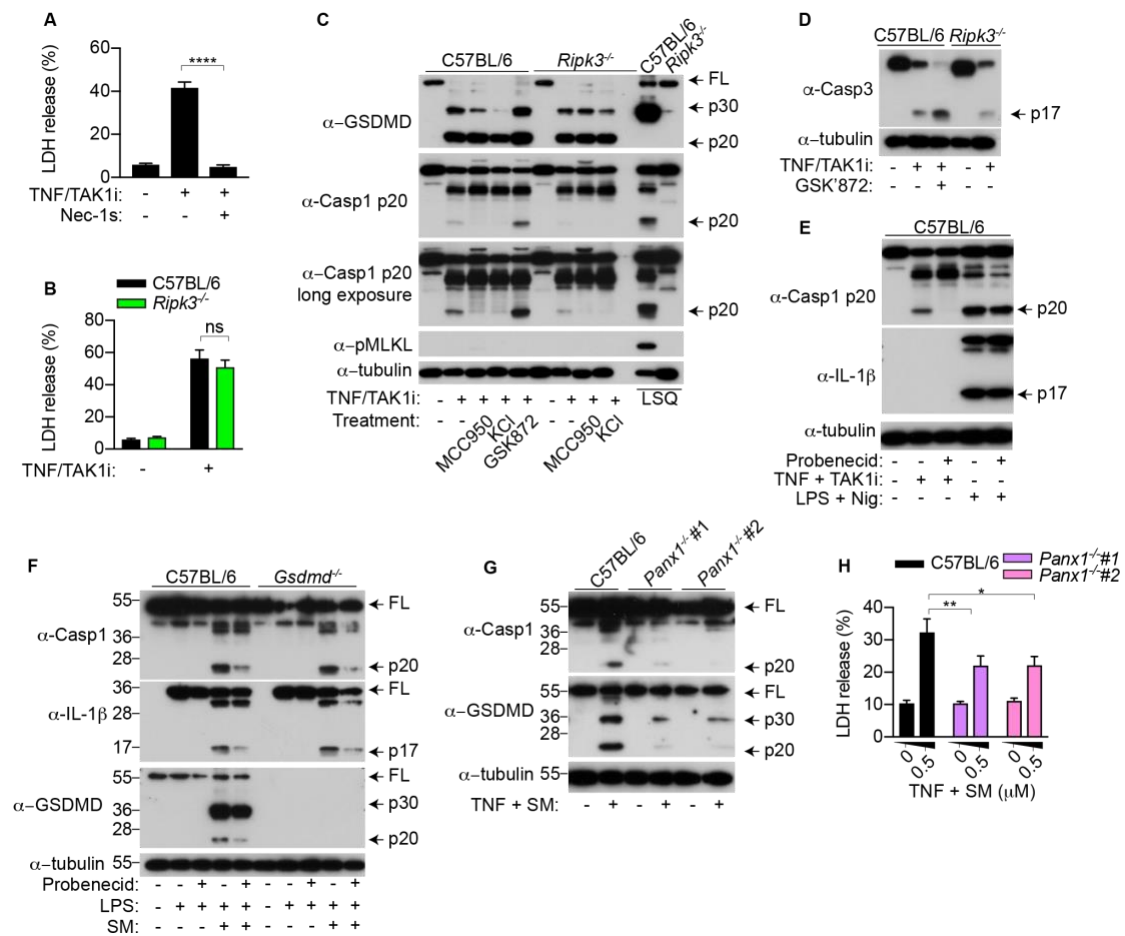


Figure 4. RIPK3 promotes caspase-3 activation and Pannexin-1 activity to drive NLRP3 assembly during extrinsic apoptosis. (A-E) BMDMs were costimulated with TNF (100 ng/ml) and TAK1i (125 nM) for 4 h and (A, B) LDH release was quantified or (C, D, E) mixed supernatant and extracts were analysed by immunoblot. Where indicated, cells were treated with the inhibitors Nec-1s (50 μM), MCC950 (10 μM), GSK'872 (1 μM), probenecid (1 mM) 20-30 min prior to cell stimulation. KCl (50 mM) was added together with TNF and TAK1i. (C) To induce necroptosis, BMDMs were primed for 3 h with ultrapure *E. coli* K12 LPS (100 ng/ml) and Q-VD-Oph (10 μM) was added at the last 20-30 min of priming and stimulated with SM (500 nM) for 4 h. (E) To activate the NLRP3 inflammasome, BMDM were primed with ultrapure *E. coli* K12 LPS (100 ng/ml) for 4 h and stimulated with nigericin (10 μM) for 1 h. (F) BMDMs were primed with for 3 h with ultrapure *E. coli* K12 LPS (100 ng/ml) and stimulated with SM (0.5 μM) for a further 4 h. Probenecid (1 mM) was added 20-30 min prior to cell stimulation and mixed supernatant and extracts

were analysed by immunoblot. (G-H) BMDMs were stimulated with TNF (100 ng/ml) and SM (0.5 μ M) for 6 h and (G) mixed supernatant and extracts were analysed by immunoblot or (H) LDH release was quantified. All immunoblots are representative of 3 independent experiments. (A, B, H) Data are means \pm SEM of pooled data from (A, H) 4 or (B) 3 independent experiments. Data were considered significant when * P <0.05, ** P <0.01 or *** P <0.0001.

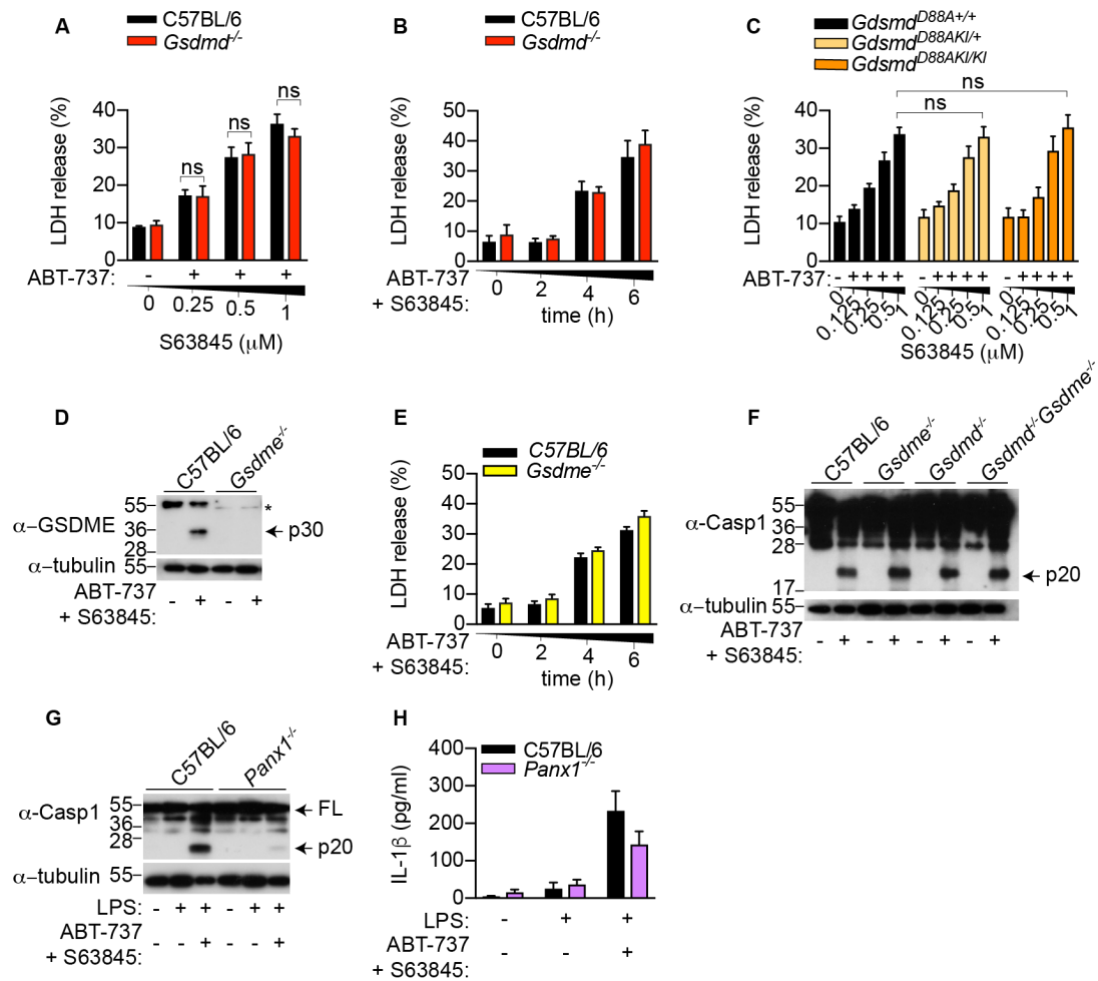
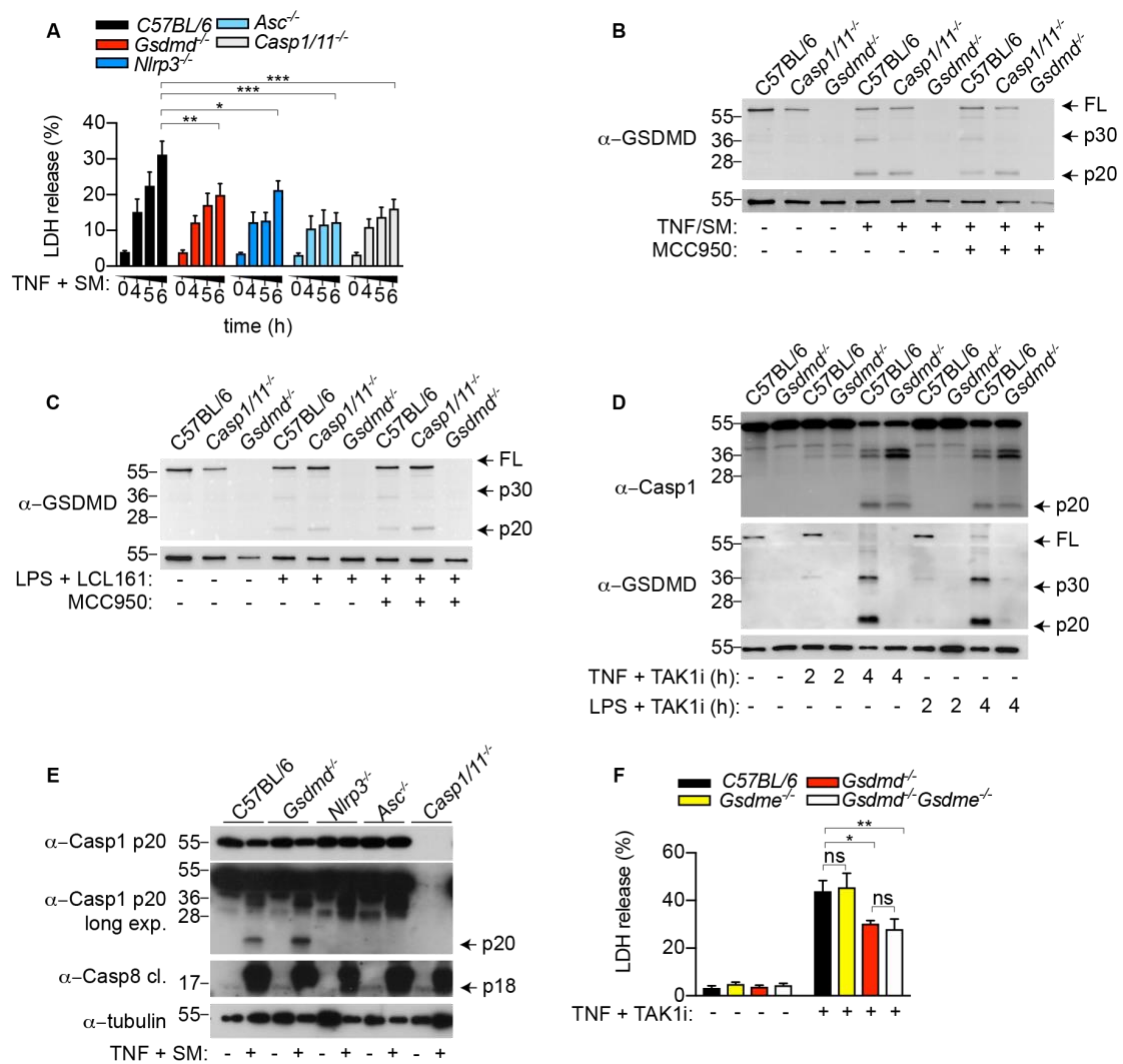


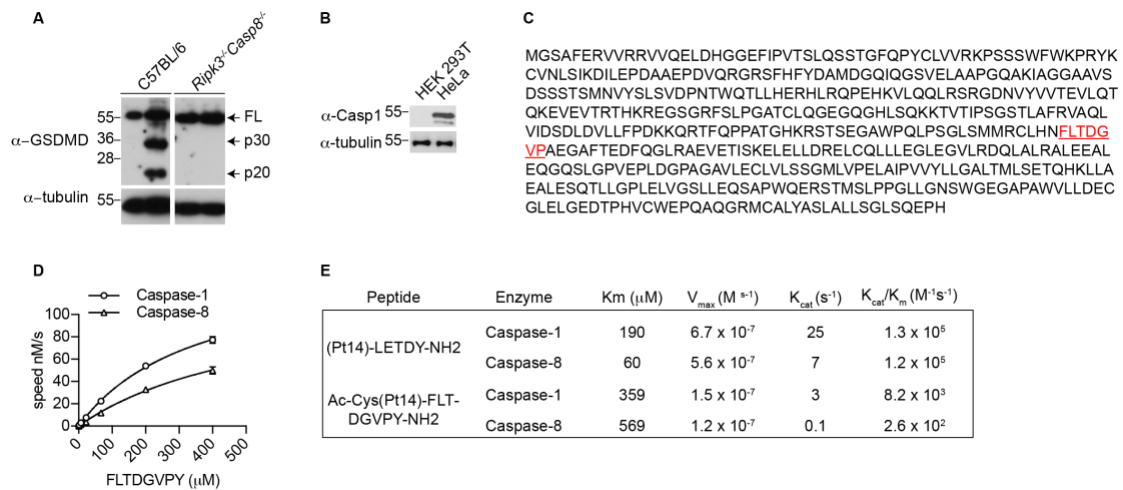
Figure 5. Intrinsic apoptosis drives gasdermin-independent cell lysis but promotes NLPR3 assembly through pannexin-1 activity. (A, C) BMDMs were stimulated with an increasing dose of S63845 in the presence of ABT-737 (0.5 μ M) and LDH release was quantified at 6 h. (B, D, E, F) BMDMs were stimulated with ABT-737 (0.5 μ M) and S63845 (0.5 μ M) and LDH release was quantified (B, D) or mixed supernatant and extracts were analysed by immunoblot at 6 h (D, F). (G-H) BMDMs were primed with ultrapure *E. coli* K12 LPS (100 ng/ml) for 3 h and further stimulated with ABT-

737 (1 μ M) and S63845 (1 μ M) for 24 h and mixed supernatant and extracts were analysed by immunoblot (G) and IL-1 β in cell-free supernatant were quantified by ELISA (H). All immunoblots are representative of 3 independent experiments. Data are means \pm SEM of pooled data from (A) 4, (B, E, H) 3 or (C) 5 independent experiments.

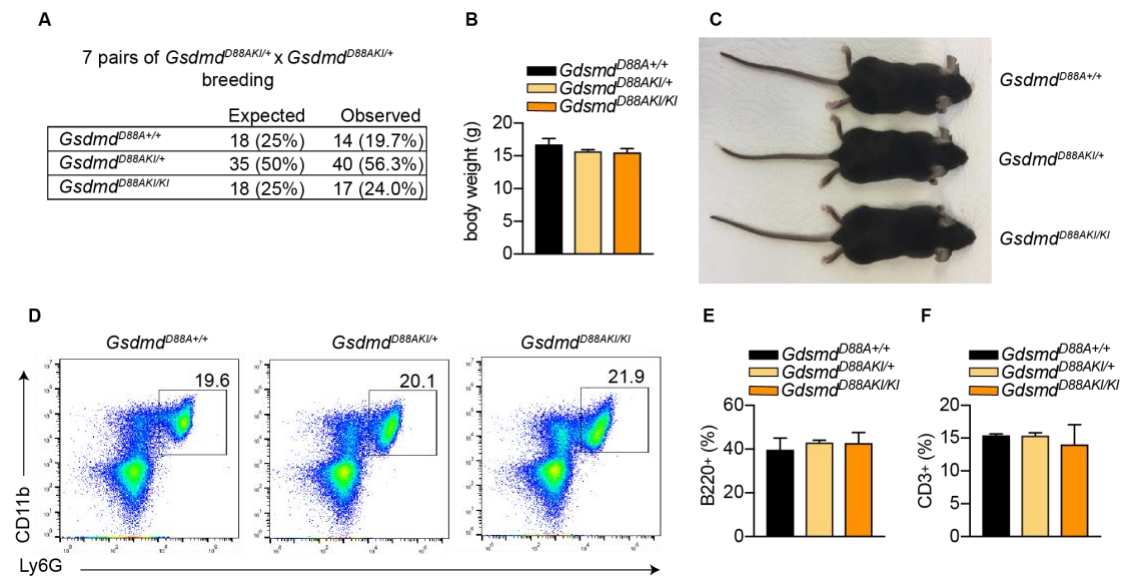


Supplementary Figure 1. Caspase-8 triggers NLRP3/caspase-1 independent GSDMD processing. (A) BMDMs were costimulated with TNF (100 ng/ml) and SM (500 nM) for the indicated time points and LDH release was quantified. (B) Immortalized or BMDM were costimulated with TNF (100 ng/ml) and SM (500 nM) for 6 h or (C) primed with ultrapure *E. coli* K12 LPS (100 ng/ml) for 3 h prior to stimulation with the SMAC mimetic LCL161 (1 μ M) for a further 16 h. Mixed supernatant and extracts were analysed by immunoblot. (D) BMDM were costimulated with ultrapure *E. coli* K12 LPS (100 ng/ml) or TNF (100 ng/ml) and TAK1i (125 nM) for 2 or 4 h and mixed supernatant and extracts were analysed by immunoblot. (E) BMDMs were costimulated with TNF (100 ng/ml) and SM (500 nM) for 6 h and mixed supernatant and extracts were analysed by immunoblot. (F) BMDMs were costimulated with TNF (100 ng/ml) and TAK1i (125 nM) and LDH release was

quantified at 4 h. Data are means +SEM of pooled data (A) 3-6 or (F) 4 from individual experiments. Data were considered significant when $*P<0.05$, $**P<0.01$, $***P<0.001$ or $****P<0.0001$. Immunoblots are representative of 2 (E) or 3 (B-D) individual experiments.

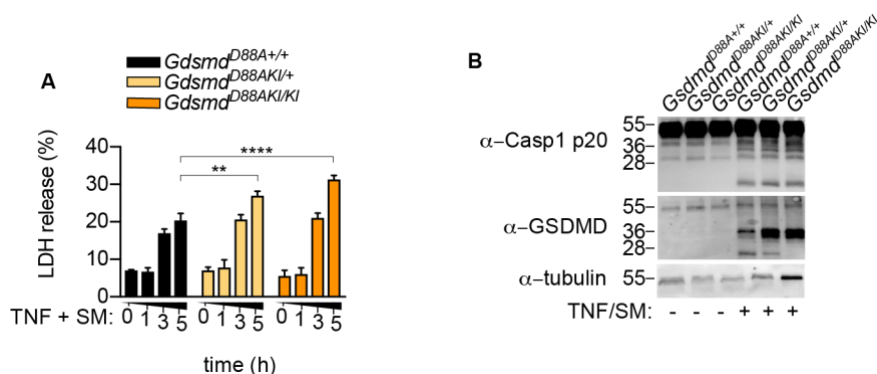


Supplementary Figure 2. Caspase-8 cleaves GSDMD at a lower efficiency than caspase-1. (A) BMDMs were stimulated with TNF (100 ng/ml) and SM (500 nM) for 6 h and mixed supernatant and extracts were analysed by immunoblot; representative of 3 independent experiments. (B) Caspase-1 expression in HEK 293T versus HeLa cells. (C) Amino acid sequence of human Gasdermin D. The fluorescence lifetime substrate Ac-Cys(Pt14)-FLTD[^]GVPY-NH2 was designed around D276 as highlighted (red); [^] indicates the Casp1/8 cleavage site. (D) The kinetic constants of the proteolysis of the FLT-substrate Ac-Cys(Pt14)-FLTD[^]GVPY-NH2 by Casp1/8 were determined from the time courses of product formation under initial velocity conditions. The K_M value was obtained from measurements conducted at constant enzyme concentration (Casp1 = 30 nM; Casp8 = 833 nM) and different substrate concentrations as indicated. (E) Comparison of kinetic constants determined for Caspase-1/8 cleavage of (Pt14)-LETD[^]Y-NH2 and Ac-Cys(Pt14)-FLTD[^]GVPY-NH2.



Supplementary Figure 3. Characterisation of the *Gsdmd*^{D88AKI/KI} mouse.

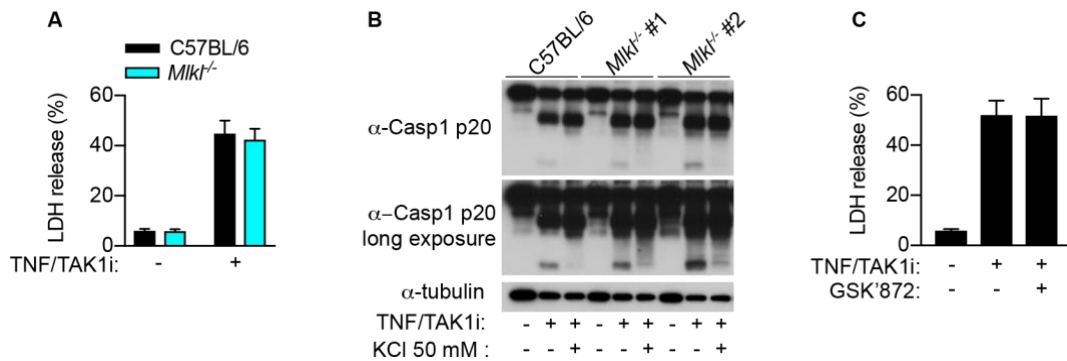
(A) Expected and observed frequency of offspring from 7 pairs of *Gsdmd*^{D88AKI/+} mating. (B) Body weight of *Gsdmd*^{D88A} litters at 5-6 weeks of age. (C) Representative image of *Gsdmd*^{D88A} littermate at 5 weeks of age. (D-F) Total bone marrow (D) or splenocytes (E-F) were stained by the indicated surface markers and analysed by flow cytometry. (D) FACS plots are representative of analysis of littermates from 3 independent breeding pairs. (B, E-F) Data are +SEM of 3-9 littermates from 2 breeding pairs.



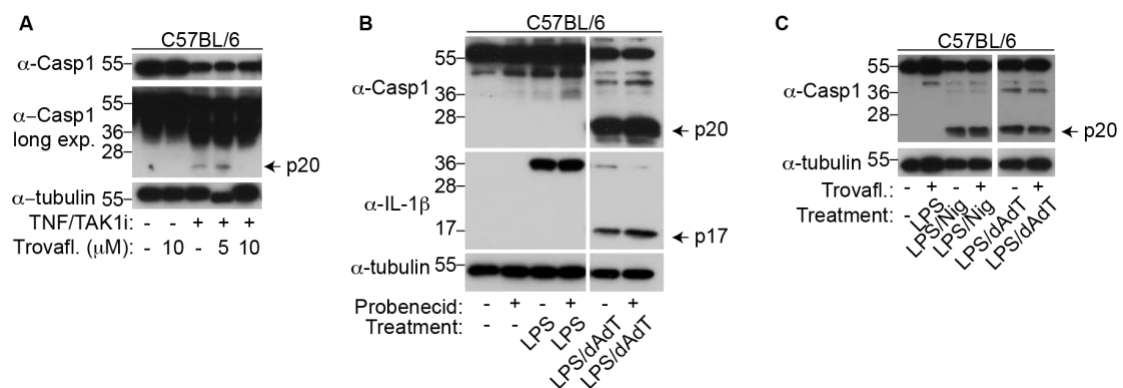
Supplementary Figure 4. *Gsdmd*^{D88AKI/KI} BMDM are more susceptible to extrinsic apoptosis.

(A-B) BMDMs were costimulated with TNF (100 ng/ml) and SM (500 nM) and (A) LDH release was quantified at the indicated time points or (B) mixed supernatant and extracts were analysed at 5 h. (A) Data are means +SEM of pooled data from 3 independent experiments. Data were

considered significant when $**P<0.01$ or $***P<0.0001$. (B) Immunoblots are representative of 3 independent experiments.

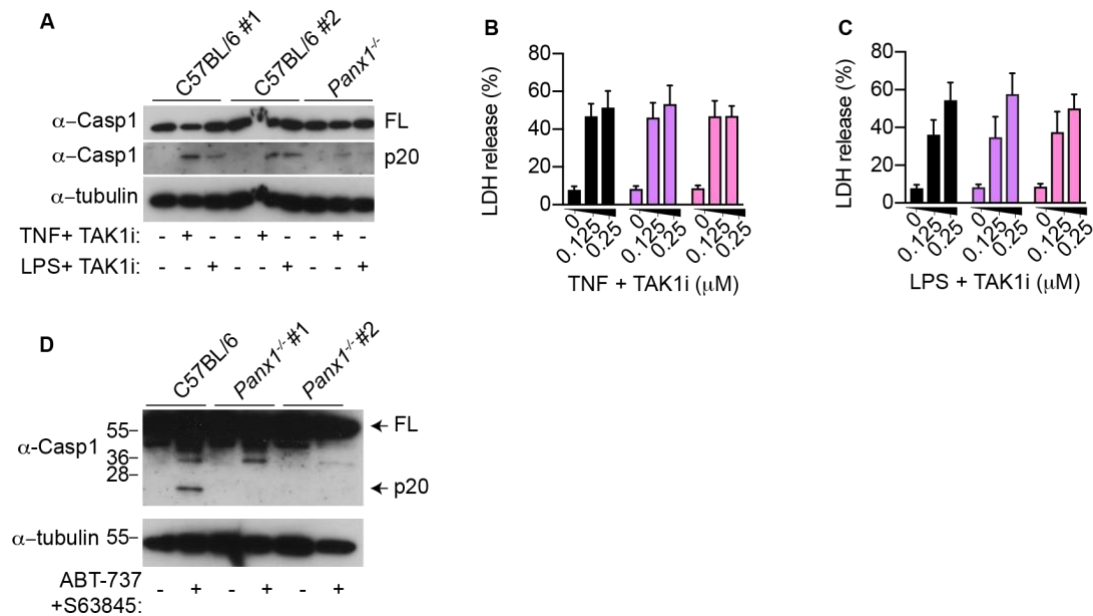


Supplementary Figure 5. TNF and TAK1i trigger RIPK3 kinase and MLKL *Mikl*-independent cell death and caspase-1 processing. (A-C) BMDMs were costimulated with TNF (100 ng/ml) and TAK1i (125 nM) and (A-C) LDH release and (B) mixed supernatant and extracts were analysed at 4 h. Where indicated, cells were treated with GSK'872 (1 μ M) 20-30 min prior to cell stimulation. KCl (50 mM) was added together with TNF and TAK1i. Data are mean + SEM of pooled data from (A) 5-9 or (C) 4 independent experiments. Immunoblots are representative of 3 independent experiments.

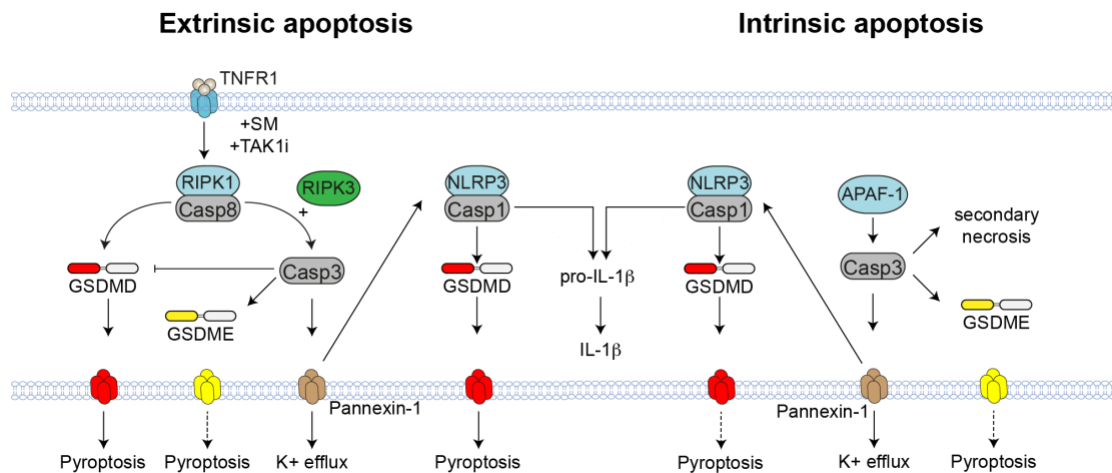


Supplementary Figure 6. Probenecid and trovafloxacin do not affect caspase-1 processing following AIM2 stimulation or NLRP3 activation. (A) TNF (100 ng/ml) and TAK1i (125 nM) for 4 h. (B-C) BMDMs were primed with for 4 h with ultrapure *E. coli* K12 LPS (100 ng/ml) and stimulated with nigericin (10 μ M) or transfected with poly(dAdT) (0.2 μ g/well). Where

indicated, probenecid (1 mM) and trovafloxacin (trovafl.; 10 μ M) were at the last 20-30 min of priming or 20-30 min before stimulation. Mixed supernatant and extracts were analysed by immunoblot. Immunoblots are representative of (A-B) 3 or (C) 2 independent experiments.



Supplementary Figure 7. Extrinsic and intrinsic apoptosis promote NLRP3 assembly through pannexin-1. (A-C) BMDMs were stimulated with TNF (100 ng/ml) or *E. coli* K12 LPS (100 ng/ml) and TAK1i (125 nM) for 4 h and mixed supernatant and extracts were analysed by immunoblot (A) or (B-C) LDH release was quantified. (D) Unprimed BMDM were stimulated with ABT-737 (500 nM) and S63845 (500 nM) for 6 h and mixed supernatant and extracts were analysed by immunoblot. Immunoblots are representative of 3 independent experiments. Data are mean + SEM of pooled data from (B-C) 4 independent experiments.



Supplementary Figure 8. Schematic for ripoptosome- and apoptosome-mediated cell death and NLRP3 activation. TNFR1 signalling in the presence of SM or TAK1i promotes the assembly of the ripoptosome, a caspase-8 activating platform. Caspase-8 triggers direct GSDMD activation to induce cell lysis, which is amplified by the NLRP3 inflammasome. The cytotoxic function of caspase-8 is suppressed by caspase-3-mediated inactivation of GSDMD. Caspase-3 cleaves GSDME, but GSDME does not contribute to cell death in BMDM. Finally, RIPK3 promotes caspase-3 activation downstream of the ripoptosome to promote Pannexin-1 activity, potassium efflux and NLRP3 activation. By contrast, GSDMD does not promote cell lysis during mitochondrial apoptosis. The related gasdermin family member, GSDME, is processed into its active form during mitochondrial apoptosis, but does not promote cell lysis. Consistent with TNF-induced apoptosis, pannexin-1 but not gasdermins promote NLRP3 activation during mitochondrial apoptosis.

References

- 1 Kayagaki, N. *et al.* Caspase-11 cleaves gasdermin D for non-canonical inflammasome signalling. *Nature* **526**, 666-671, doi:10.1038/nature15541 (2015).
- 2 Shi, J. *et al.* Cleavage of GSDMD by inflammatory caspases determines pyroptotic cell death. *Nature* **526**, 660-665, doi:10.1038/nature15514 (2015).
- 3 He, W. T. *et al.* Gasdermin D is an executor of pyroptosis and required for interleukin-1 β secretion. *Cell Res* **25**, 1285-1298, doi:10.1038/cr.2015.139 (2015).
- 4 Feoktistova, M. *et al.* cIAPs block Ripoptosome formation, a RIP1/caspase-8 containing intracellular cell death complex differentially regulated by cFLIP isoforms. *Mol Cell* **43**, 449-463, doi:10.1016/j.molcel.2011.06.011 (2011).
- 5 Tenev, T. *et al.* The Ripoptosome, a signaling platform that assembles in response to genotoxic stress and loss of IAPs. *Mol Cell* **43**, 432-448, doi:10.1016/j.molcel.2011.06.006 (2011).
- 6 Vince, J. E. *et al.* Inhibitor of apoptosis proteins limit RIP3 kinase-dependent interleukin-1 activation. *Immunity* **36**, 215-227, doi:10.1016/j.immuni.2012.01.012 (2012).
- 7 Yabal, M. *et al.* XIAP restricts TNF- and RIP3-dependent cell death and inflammasome activation. *Cell Rep* **7**, 1796-1808, doi:10.1016/j.celrep.2014.05.008 (2014).
- 8 Dondelinger, Y. *et al.* NF-kappaB-Independent Role of IKK α /IKK β in Preventing RIPK1 Kinase-Dependent Apoptotic and Necroptotic Cell Death during TNF Signaling. *Mol Cell* **60**, 63-76, doi:10.1016/j.molcel.2015.07.032 (2015).
- 9 Ding, J. *et al.* Pore-forming activity and structural autoinhibition of the gasdermin family. *Nature* **535**, 111-116, doi:10.1038/nature18590 (2016).
- 10 Liu, X. *et al.* Inflammasome-activated gasdermin D causes pyroptosis by forming membrane pores. *Nature* **535**, 153-158, doi:10.1038/nature18629 (2016).
- 11 Sborgi, L. *et al.* GSDMD membrane pore formation constitutes the mechanism of pyroptotic cell death. *EMBO J* **35**, 1766-1778, doi:10.15252/embj.201694696 (2016).
- 12 Aglietti, R. A. *et al.* GsdmD p30 elicited by caspase-11 during pyroptosis forms pores in membranes. *Proc Natl Acad Sci U S A* **113**, 7858-7863, doi:10.1073/pnas.1607769113 (2016).
- 13 Chen, K. W. *et al.* Noncanonical inflammasome signaling elicits gasdermin D-dependent neutrophil extracellular traps. *Sci Immunol* **3**, doi:10.1126/sciimmunol.aar6676 (2018).
- 14 Sollberger, G. *et al.* Gasdermin D plays a vital role in the generation of neutrophil extracellular traps. *Sci Immunol* **3**, doi:10.1126/sciimmunol.aar6689 (2018).
- 15 Taabazuing, C. Y., Okondo, M. C. & Bachovchin, D. A. Pyroptosis and Apoptosis Pathways Engage in Bidirectional Crosstalk in Monocytes and Macrophages. *Cell Chem Biol* **24**, 507-514 e504, doi:10.1016/j.chembiol.2017.03.009 (2017).
- 16 Wang, L., Du, F. & Wang, X. TNF- α induces two distinct caspase-8 activation pathways. *Cell* **133**, 693-703, doi:10.1016/j.cell.2008.03.036 (2008).

- 17 Dondelinger, Y. *et al.* RIPK3 contributes to TNFR1-mediated RIPK1 kinase-dependent apoptosis in conditions of cIAP1/2 depletion or TAK1 kinase inhibition. *Cell Death Differ* **20**, 1381-1392, doi:10.1038/cdd.2013.94 (2013).
- 18 Chen, K. W. *et al.* Cutting Edge: Blockade of Inhibitor of Apoptosis Proteins Sensitizes Neutrophils to TNF- but Not Lipopolysaccharide-Mediated Cell Death and IL-1beta Secretion. *J Immunol* **200**, 3341-3346, doi:10.4049/jimmunol.1701620 (2018).
- 19 Lawlor, K. E. *et al.* RIPK3 promotes cell death and NLRP3 inflammasome activation in the absence of MLKL. *Nat Commun* **6**, 6282, doi:10.1038/ncomms7282 (2015).
- 20 Conos, S. A. *et al.* Active MLKL triggers the NLRP3 inflammasome in a cell-intrinsic manner. *Proc Natl Acad Sci U S A* **114**, E961-E969, doi:10.1073/pnas.1613305114 (2017).
- 21 Kayagaki, N. *et al.* Non-canonical inflammasome activation targets caspase-11. *Nature* **479**, 117-121, doi:10.1038/nature10558 (2011).
- 22 Ruhl, S. & Broz, P. Caspase-11 activates a canonical NLRP3 inflammasome by promoting K(+) efflux. *Eur J Immunol* **45**, 2927-2936, doi:10.1002/eji.201545772 (2015).
- 23 Rogers, C. *et al.* Cleavage of DFNA5 by caspase-3 during apoptosis mediates progression to secondary necrotic/pyroptotic cell death. *Nat Commun* **8**, 14128, doi:10.1038/ncomms14128 (2017).
- 24 Wang, Y. *et al.* Chemotherapy drugs induce pyroptosis through caspase-3 cleavage of a gasdermin. *Nature* **547**, 99-103, doi:10.1038/nature22393 (2017).
- 25 Orning, P. *et al.* Pathogen blockade of TAK1 triggers caspase-8-dependent cleavage of gasdermin D and cell death. *Science*, doi:10.1126/science.aau2818 (2018).
- 26 Gutierrez, K. D. *et al.* MLKL Activation Triggers NLRP3-Mediated Processing and Release of IL-1beta Independently of Gasdermin-D. *J Immunol* **198**, 2156-2164, doi:10.4049/jimmunol.1601757 (2017).
- 27 Moriwaki, K., Bertin, J., Gough, P. J. & Chan, F. K. A RIPK3-caspase 8 complex mediates atypical pro-IL-1beta processing. *J Immunol* **194**, 1938-1944, doi:10.4049/jimmunol.1402167 (2015).
- 28 Chekeni, F. B. *et al.* Pannexin 1 channels mediate 'find-me' signal release and membrane permeability during apoptosis. *Nature* **467**, 863-867, doi:10.1038/nature09413 (2010).
- 29 Yang, D., He, Y., Munoz-Planillo, R., Liu, Q. & Nunez, G. Caspase-11 Requires the Pannexin-1 Channel and the Purinergic P2X7 Pore to Mediate Pyroptosis and Endotoxic Shock. *Immunity* **43**, 923-932, doi:10.1016/j.immuni.2015.10.009 (2015).
- 30 Silverman, W., Locovei, S. & Dahl, G. Probenecid, a gout remedy, inhibits pannexin 1 channels. *Am J Physiol Cell Physiol* **295**, C761-767, doi:10.1152/ajpcell.00227.2008 (2008).
- 31 Poon, I. K. *et al.* Unexpected link between an antibiotic, pannexin channels and apoptosis. *Nature* **507**, 329-334, doi:10.1038/nature13147 (2014).
- 32 Chauhan, D. *et al.* BAX/BAK-Induced Apoptosis Results in Caspase-8-Dependent IL-1beta Maturation in Macrophages. *Cell Rep* **25**, 2354-2368 e2355, doi:10.1016/j.celrep.2018.10.087 (2018).
- 33 Vince, J. E. *et al.* The Mitochondrial Apoptotic Effectors BAX/BAK Activate Caspase-3 and -7 to Trigger NLRP3 Inflammasome and Caspase-8 Driven IL-

1beta Activation. *Cell Rep* **25**, 2339-2353 e2334,
doi:10.1016/j.celrep.2018.10.103 (2018).

34 Ahmad, K. Drug company sued over research trial in Nigeria. *Lancet* **358**,
815, doi:10.1016/S0140-6736(01)06011-1 (2001).